

# We are IntechOpen, the world's leading publisher of Open Access books Built by scientists, for scientists

6,900

Open access books available

186,000

International authors and editors

200M

Downloads

Our authors are among the

154

Countries delivered to

TOP 1%

most cited scientists

12.2%

Contributors from top 500 universities



WEB OF SCIENCE™

Selection of our books indexed in the Book Citation Index  
in Web of Science™ Core Collection (BKCI)

Interested in publishing with us?  
Contact [book.department@intechopen.com](mailto:book.department@intechopen.com)

Numbers displayed above are based on latest data collected.  
For more information visit [www.intechopen.com](http://www.intechopen.com)



# Coherent Optical Phonons in Bismuth Crystal

Davide Boschetto and Antoine Rousse

*Laboratoire d'Optique Appliquée, ENSTA ParisTech/Ecole Polytechnique/CNRS, Chemin de la Hunière, 91761 Palaiseau cedex France*

## 1. Introduction

This chapter is devoted to the study of the lattice vibrations within a crystal structure using laser-based time resolved spectroscopic methods. We have used ultrafast pulsed laser systems to extend the analysis of atomic displacements into the time domain with femtosecond resolution. This field has gained a lot of attention from a large scientific community during the past decades. Actually, the knowledge of all the properties in a crystal depends on two key factors: the way in which atoms arrange themselves to give rise to the crystal structure, and the movement of both electrons and atoms within this structure. Many physical parameters, such as the transport properties, strongly depend on the dynamical behavior of both electrons and atoms. Besides, the mutual interaction between them determines the pathway of chemical reactions and phase transitions. As an example, one challenge in solid state physics is the understanding and control of high temperature superconductivity, in which the dynamical aspect may play a crucial role. If there is a lattice displacement responsible for the Cooper pairs formation, its selective excitation could be exploited to reach a superconductivity phase even at temperature well above the known transition temperature. The general question is how can we modify the phase of a material using photons. This type of studies belong to a broader research area, known as the science of photoinduced phase transition. An important point is that high frequency lattice vibrations are the first response of ions to the external pumping laser pulse. Therefore, the study of such movements could clarify the energy relaxation channels of the excess energy stored into the electrons subsystem from the pumping laser pulse.

Another important application of the study of coherent phonon concerns nanostructures. When reducing the size down to the nanometric scale, the ratio between the atomic displacement and the structure size increases considerably. Together with the confinement effect, this produces major modifications of the physical properties.

The general movement of the atoms within the crystal structure can be seen as an elastic deformation, which can be described as a sum of several normal modes of vibration of the lattice. The quantum of energy associated to a normal mode of vibration of the lattice is called phonon. In order to study each of these elementary vibrations, there is a need to excite and detect selectively the desired phonon mode. This is possible only if we can excite and detect the phonon mode coherently, i.e. the atomic vibration has a given phase which is kept in a time window, called the dephasing time or damping time.

Coherent phonons were observed in many different materials, and their extensive study in novel materials represents a large part of the activity centered on the femtosecond laser

applications. Here, we will focus our attention on bismuth crystal mainly because it is the simplest case for which the description approaches the ideal situation of a single harmonic oscillator. This will allow an understanding of the key points in coherent phonons studies.

This chapter is structured as follows. First, we will define the main properties of coherent phonons, highlighting the difference between coherent and incoherent phonons. We will then address the question of how to excite and detect a coherent phonon, focussing on the different optical properties. The dependence of phonon parameters in bismuth crystals on several factors such like excitation fluence and lattice temperature will be discussed.

## 2. Coherent and incoherent phonons

It is well known that atoms in the lattice vibrate around their equilibrium positions, with a vibration amplitude that increases with temperature. Such vibrations can be decomposed in a sum of normal modes, which depend on the symmetry of the lattice. The quantum of energy associated to the vibration of a given normal mode is called phonon (Ashcroft and Mermin, 1976).

The temperature effect results in an incoherent movement of the atoms in the lattice, in which each atom vibrates independently. In this case there is no phase relationship between the vibration of each atom. We call these incoherent phonons. Instead, in the case of a coherent phonon, there is a well defined phase relationship, and the generic  $i$ th atom moves following a sinusoidal function  $\sin(\omega t - \vec{k} \cdot \vec{x}_i + \phi)$ , where  $t$  is the time,  $\omega$  and  $\vec{k}$  are the vibration frequency and wavevector, respectively,  $\phi$  is the initial phase and  $\vec{x}_i$  is the position of the  $i$ th atom in the lattice.

The difference between a coherent and an incoherent phonon can be visualized thinking of the sea surface. Without perturbations, the surface of the sea is modulated by several waves, which sum to each other. This gives rise to the well known sea surface fluctuations, where each part of the surface can vibrate independently from their neighbors. This is an incoherent movement at the surface of the sea, which could be associated to the incoherent phonons. On the other hand, we all know that when a boat comes across the sea, it generates a wave form modulation of the sea surface, whose spatial frequency and amplitude depends for example on the speed and the size of the boat. This wave generates a modulation of the sea surface which propagates as a coherent wave, which can be associated to coherent phonons. We will see in the following that the laser pulse propagating into the crystal plays the same role than the boat on the surface of the sea.

Only coherent optical phonons will be discussed in this chapter. First, optical phonons are the first response of the lattice to the external laser pulse excitation, mainly because they are generated much more rapidly due to their much higher vibration frequency near the center of the Brillouin zone. Moreover, the optical phonons represent the movement of the atoms within the elementary cell, and can be regarded as the elementary atomic movement.

In the most general way, a coherent optical phonon displacement must be described as the following

$$Q(t) = A_{ph} e^{-t/\tau} \sin(\omega t - \vec{k} \cdot \vec{x}_i + \phi) \quad (1)$$

where  $A_{ph}$  is the phonon amplitude and  $\tau$  is the phonon damping time. As it will be shown, laser pulse excitation produces phonons whose wavevector is always very close to zero, therefore we will neglect it hereafter. Instead, the parameters of interest in the study of

coherent phonon are the amplitude, the frequency and the damping time. On the other hand, the initial phase is often used to discriminate between the different excitation mechanisms.

### 3. Excitation and detection of coherent optical phonons

In order to study the dynamical behavior of a given phonon mode two key factors are required. We must be able to excite coherently the phonon we are interested in, and we must be able to detect the corresponding atomic displacements. The pump probe technique using the very high time resolution of modern laser systems is a unique tool for this purpose. The excitation and detection mechanisms are independent, so it is possible to excite the coherent phonon using one laser pulse and detect it using any other pulse of the desired wavelength, from hard X-ray to infrared spectral range. We will first describe the excitation of coherent optical phonon by a laser pulse in visible and near infrared range, and then show how the detection can be done from reflectivity measurements.

#### 3.1 Excitation mechanisms

The excitation of a coherent optical phonon can be viewed in a classical frame by considering the case of a forced harmonic oscillator, which follows the equation

$$\frac{d^2Q(t)}{dt^2} + \frac{2}{\tau} \frac{dQ(t)}{dt} + \omega^2 Q(t) = \frac{F(t)}{m} \quad (2)$$

where the applied external force  $F(t)$  is due to the pumping laser pulse. All the existing mechanisms used to describe the excitation of coherent phonon are focussed on the expression of the driving force. We can distinguish mainly three mechanisms, the impulsive stimulated Raman scattering (ISRS) (Yan, 1985), the theory of displacive excitation of coherent phonon (DECP) (Zeiger, 1992) and the temperature gradient theory (TGT) (Garl, 2008, a). Before going into the summary description of each of these models, we must recall some fundamental experimental results. In the case of a transparent material, the phonon excitation and detection follows the Raman selection rules, therefore providing an experimental evidence that the excitation mechanism is probably a pure stimulated Raman process. Instead, in the case of opaque materials, only the completely symmetric optical phonons are observed, namely the  $A_{1g}$  mode (Zeiger, 1992), if they exist, even when the Raman cross section associated with the  $A_{1g}$  phonon is much lower than the other modes with different symmetry. The case of superconductor iron pnictide is a great example of this (Mansart, 2009). In pump probe experiments on opaque materials, phonons modes other than  $A_{1g}$  were detected only at low temperature (Ischioka, 2006). The only exception is the case of graphite (Ischioka, 2008), in which the shearing mode with  $E_{1g}$  symmetry can be excited with higher efficiency with respect to the  $A_{1g}$  mode.

##### 3.1.1 Impulsive stimulated Raman scattering

Let's suppose that the crystal under study is transparent and has a Raman active mode of frequency  $\omega$ , and that we let propagate into the crystal two laser pulses with frequency and wavevector  $(\omega_1, \vec{k}_1)$  and  $(\omega_2, \vec{k}_2)$ , respectively. If the following relation is satisfied

$$\omega_1 - \omega_2 = \omega \quad (3)$$

the phonon with frequency  $\omega$  will be excited into the crystal, with a wavevector given by the phase matching condition

$$\vec{k} = \vec{k}_1 - \vec{k}_2 \quad (4)$$

As a laser pulse is usually in the visible or near infrared range, the corresponding wavevector is orders of magnitude smaller than the edge of the Brillouin zone, therefore the excited phonon wavevector is close to the  $\Gamma$  point and can be approximated by zero.

In the case of a short laser pulse, the spectral shape can be large enough so that the two frequencies  $\omega_1$  and  $\omega_2$  are within the same pulse, and therefore the phonon can be excited by only one laser pulse.

The key hypothesis of the ISRS theory (Yan, 1985; Merlin, 1997) is that the polarizability  $\alpha$  is not constant, but rather depends on the relative distance between the atoms and therefore on the phonon displacement (Boyd, 2003)

$$\alpha(t) = \alpha_0 + \left( \frac{\partial \alpha(t)}{\partial Q} \right)_0 \cdot Q(t) \quad (5)$$

where  $\alpha_0$  is the polarizability corresponding to the equilibrium position. The external force acting in equation 2 can be written as (Yan, 1985)

$$F(t) = \frac{1}{2} N \left( \frac{\partial \alpha(t)}{\partial Q} \right)_0 : \vec{E} \cdot \vec{E} \quad (6)$$

where  $\vec{E}$  is the optical electric field and  $N$  is the volume density of oscillators. If  $\tau \gg \omega$ , the solution of the equation 2 is

$$Q(z > 0, t > 0) = Q_0 e^{-\frac{1}{\tau}(t - \frac{zn}{c})} \sin \left[ \omega \left( t - \frac{zn}{c} \right) \right] \quad (7)$$

where  $z$  is the propagation direction of the laser. It is possible to show that the phonon amplitude  $Q_0$  is proportional to  $e^{-\omega^2 \tau_L^2 / 4}$  where  $\tau_L$  is the laser pulse duration. Therefore, the maximum phonon amplitude is reached when the following condition is satisfied

$$\tau_L \ll \frac{2\pi}{\omega} \quad (8)$$

This condition is called the *impulsive limit*. Obviously, when  $\tau_L \gg 2\pi/\omega$ ,  $Q_0 \sim 0$ .

We point out that this theory is in perfect agreement with all the existing experimental results on transparent materials. Instead, for opaque materials, an extension of the ISRS was made by (Stevens, 2002) by proving that the stimulated Raman scattering is defined rather by two different tensors instead of one, having the same real parts but distinct imaginary parts in the absorbing region. This model was successfully applied to the case of *Sb*.

### 3.1.2 Theory of displacive excitation of coherent phonon

The theory of displacive excitation of coherent phonon (DECP) (Zeiger, 1992) was developed to address the case of absorbing material, in which only the  $A_{1g}$  mode was observed, regardless to the value of the Raman tensor coefficients. The key point of this theory is that the laser pulse, affecting both the density of electrons in the conduction band and their temperature, results in an abrupt change in the equilibrium position of the atoms within the elementary cell and produces an atomic displacement that sets up the oscillations of the atoms around their new equilibrium positions. By assuming that the main effect of the laser pulse is the excitation of electrons from the valence to the conduction band, the external force in equation 2 is

$$F(t) = \omega^2 \kappa j(t) \quad (9)$$

where  $\kappa$  is a constant and  $j(t)$  is the density of electrons in the conduction band.

If  $\tau \gg \frac{2\pi}{\omega}$  and  $\tau_L \ll \frac{2\pi}{\omega}$ , the solution of equation 2 is

$$Q(t > 0) = Q_0 \left[ e^{-\beta t} - e^{-\frac{t}{\tau}} \cos(\omega t + \phi) \right] \quad (10)$$

where  $\beta$  is the electrons decay rate. This theory explains the unique excitation of  $A_{1g}$  mode on the basis of thermodynamics arguments.

### 3.1.3 Temperature gradient theory

This theory approaches the excitation of coherent phonon from an analysis of all the forces acting into the crystal when the interaction with the laser pulse occurs (Garl, 2008, b). Three types of forces can be recognized, namely the ponderomotive force, the polarization force analog to Raman scattering process, and the thermal force, produced by the thermal gradients of both of electrons and lattice. Therefore

$$F(t) = F^{pond} + F^{pol} + F^{grad} \quad (11)$$

The key point is that a quantitative analysis shows that the force due to gradient temperature is the largest, and therefore excites the coherent phonons.

### 3.2 Electrons and lattice temperature in photoexcited absorbing crystal

In absorbing material, the interaction with the laser pulse produces several effects, which could be described looking at the time scale on which these effects take place, as shown in figure 1 (Boschetto, 2010, a). The laser pulse energy is first stored into the electrons, causing changes in free carriers density as well as in their temperature. We must point out here that the word *temperature* must be taken carefully. Actually, we usually talk about temperature only if the distribution of kinetic energy follows a maxwellian distribution. This happens once the system reaches an equilibrium condition, which could be stable, i.e. not changing in time, or metastable, therefore evolving in time. If the collision time between the particles is short enough in comparison to the time scale under study, the particles subsystem, in our case electrons or phonons, are in equilibrium and therefore we could define a temperature for each subsystem. What happens when the distribution in kinetic energy is not maxwellian goes beyond the scope of this chapter. The pump pulse is exponentially absorbed at the surface of the crystal, generating therefore a gradient in electrons temperature along the direction of propagation of the light. At this stage, we can therefore define two temperatures independently. On one hand, the electrons temperature, and on the other hand the lattice temperature. On a time scale shorter than the electron phonon coupling time, the electrons did not have enough time to exchange their energy with the lattice.

Therefore, the lattice is at room temperature whereas the electrons reach very high temperature because of their low heat capacity. Once the electrons are excited, they start sharing their energy with the lattice through electron phonon coupling. The time required for the electrons and phonons subsystem to equilibrate can be calculated by using the two temperatures model (Anisimov, 1975). In this model, we consider that the energy exchange between electrons and phonons scales linearly with the temperature difference between these two subsystems. The two coupled differential equations describing the evolution of the electrons and lattice temperature, namely  $T_e$  and  $T_l$ , in both space and time are (Anisimov, 1975)

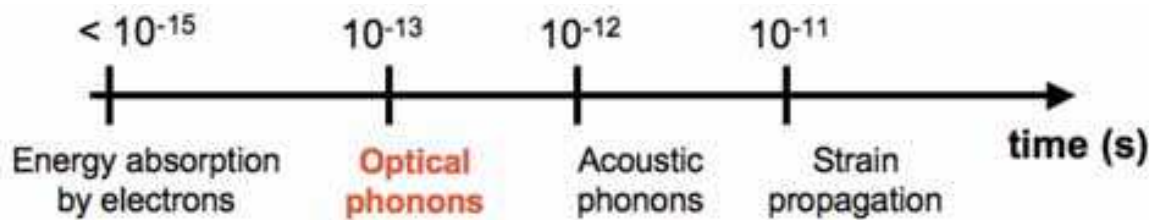


Fig. 1. Time scales of several processes taking place when a femtosecond pulse excites a crystal, reprinted by permission of the publisher (Taylor & Francis Ltd, <http://www.tandf.co.uk/journals>) from (Boschetto, 2010 , a).

$$\begin{aligned} C_e \frac{\partial T_e}{\partial t} &= \frac{\partial}{\partial z} \left( \kappa_e \frac{\partial T_e}{\partial z} \right) - g(T_e - T_l) + P(z,t) \\ C_l \frac{\partial T_l}{\partial t} &= g(T_e - T_l) \end{aligned} \tag{12}$$

where  $C_e$  and  $C_l$  are the heat capacities of electrons and lattice, respectively,  $\kappa_e$  is the electrons thermal conductivity,  $g$  is the electrons phonons coupling constant and  $P(z,t)$  is the absorbed energy density. Here we neglected the lattice thermal diffusion, which takes place on a much longer time scale with respect to the temporal ranges presented in this chapter. If the electron diffusion is a very slow process with respect to the electrons phonons equilibration time, the final lattice temperature in the skin depth can be calculated simply by the requirement of energy conservation. In the opposite case, the excess energy stored in the electrons subsystem will escape from the skin depth, therefore resulting in a lower lattice temperature.

3.3 Transient reflectivity in absorbing crystal

In the previous paragraphs we have seen that the interaction of the femtosecond pump laser pulse with absorbing crystal will generate a modification in electrons and lattice temperature, as well as will excite one or more coherent phonon displacements. If the dielectric constant is modified by these changes, the signature of each of these effects should show up in the transient reflectivity. A general approach to the description of the transient reflectivity in absorbing materials, regardless to the mechanism invoked for coherent phonon excitation, was developed in reference (Boschetto, 2008 , a). We will give here the major outlines. The reflectivity depends on the real and imaginary part of the dielectric constant, namely  $\epsilon_{Re}$  and  $\epsilon_{Im}$ , through the well known Fresnel formula. The point is now to evaluate the way in which the dielectric constant changes when a coherent phonon mode is set up into the crystal, as well as its dependence on electrons and lattice temperature. For sake of simplicity, let's assume that the dielectric constant of the crystal under study can be well described by the Drude model (Ashcroft and Mermin, 1976)

$$\begin{aligned} \epsilon_{Re} &= 1 - \frac{\omega_p^2}{\omega_l^2 + \nu_{e-ph}^2} \\ \epsilon_{Im} &= \frac{\omega_p^2}{\omega_l^2 + \nu_{e-ph}^2} \frac{\nu_{e-ph}}{\omega_l} \end{aligned} \tag{13}$$

where  $\omega_l$  and  $\omega_p$  are the laser frequency and the plasma frequency, respectively, whereas  $\nu_{e-ph}$  is the electron phonon collision frequency. The plasma frequency is defined as a function of the effective electron mass  $m_e$ , the electron charge  $e$  and the free carriers density  $n_e(t)$  as the following

$$\omega_p^2 = \frac{4\pi e^2 n_e(t)}{m_e^*} \quad (14)$$

The key point of this approach is that the electron phonon collision frequency can be expressed in the frame of the kinematical theory as (Ziman, 2004)

$$\nu_{e-ph} = \sigma_{e-ph} n_{ph} v_e \quad (15)$$

where  $\sigma_{e-ph}$  is the electron phonon scattering cross section,  $n_{ph}$  is the phonon density and  $v_e$  is the electron velocity. Knowing that

$$n_{ph} \cong \frac{n_a T_L(t)}{T_D} \quad (16)$$

where  $n_a$  is the atoms density in the crystal and  $T_D$  is the Debay temperature, and assuming a circular scattering cross section, the change in the electron phonon collision frequency due to the coherent phonon can be expressed as

$$\frac{\Delta \nu_{e-ph}}{\nu_{e-ph}^0} = \frac{\Delta T_L}{T_0} + 2 \frac{\Delta Q(t)}{Q_0} \quad (17)$$

where  $T_0$  and  $Q_0$  are the lattice temperature and phonon displacement at equilibrium before the pump pulse interact with the crystal. By taking

$$\Delta n_e(t) \propto T_e(t) \quad (18)$$

we can write the changes in transient reflectivity as the following (Boschetto, 2008 , a)

$$\frac{\Delta R}{R} = A_e T_e(t) + A_L T_L(t) + A_{ph} Q(t) \quad (19)$$

where  $A_e$ ,  $A_L$  and  $A_{ph}$  are constant which depend on the value of the partial derivatives of the reflectivity with respect to the real and imaginary part of the dielectric function as well as on the probe pulse wavelength. The algebraic sign of these constants can be different, implying a competition in the induced reflectivity changes produced by the electrons and lattice temperature. After the pump pulse arrival, the electrons temperature reaches the maximum, whereas the lattice is still cold. As described in equation 12, for longer time delay the electrons temperature decreases whereas the lattice temperature increases, until they have the same temperature, and the equilibrium is reached. Therefore, we must expect a transient behavior in the reflectivity while the two temperatures are changing, and we expect a plateau in the reflectivity when the equilibrium is reached.

### 3.4 Set up for coherent optical phonon study

The study of coherent optical phonon in time domain requires the use of ultrafast laser pulses, typical of 50 fs or less, depending on the phonon frequency under investigation. Obviously, the higher the phonon frequency the higher time resolution is required. Such a study is usually performed in a pump probe set up, summarized in figure 2.

The basic idea is that one pulse is used to excite the sample, whereas a second pulse is used to probe it. A controlled delay stage between the two beams allows to probe the sample at any given time delay from the pump arrival on the sample. The pump and probe wavelength can be different (Papalazarou, 2008). If the probe is in the visible range, we usually measure



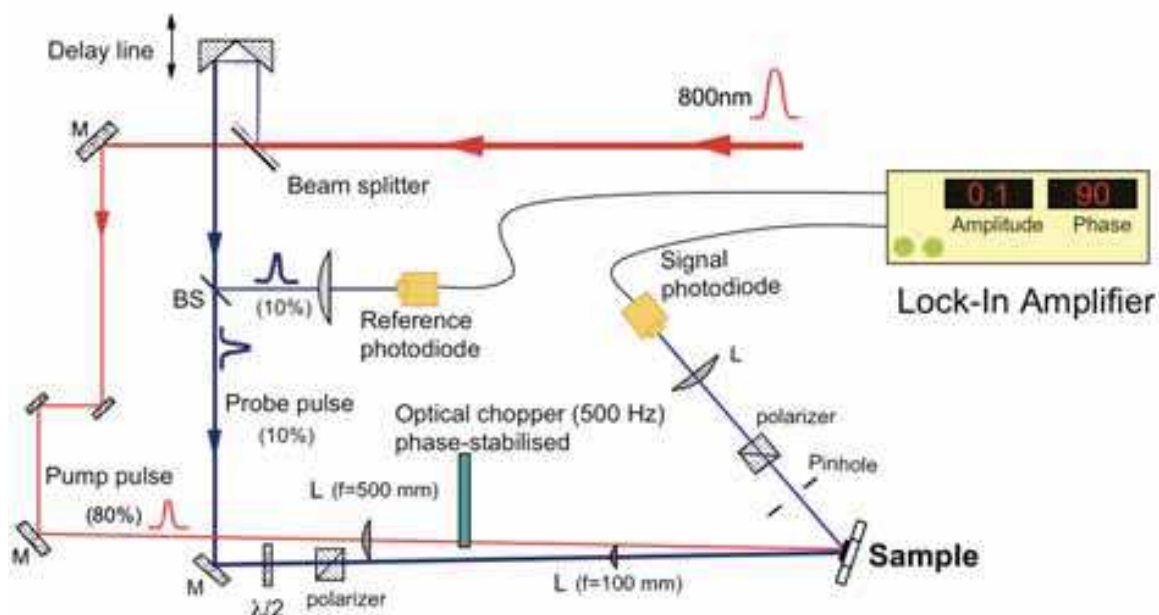


Fig. 2. Example of experimental set up for pump and probe measurement in reflectivity.

either the induced changes in reflectivity or in transmission of the sample. If the probing wavelength is in the hard X-ray range, a diffraction pattern could be recorded and analyzed at different time delay (Sokolowski, 2003; Beaud, 2007; Rousse, 2001). Here, we will focus mainly on pump probe experiments using one laser pulse at a given wavelength for recovering the transient reflectivity (Boschetto, 2008, a). In this case, a laser beam is split into two parts, one is used as pump pulse and the other as probe pulse. Eventually, the relative polarisation is changed to match the Raman selection rule for the phonon under study. The excitation of coherent optical phonon requires some attention with respect to the fluency used in the experiment. Typically, they show up only in a certain range of pump fluency, depending on the sample as well as on the pump wavelength. However, the most sensible part of the experiment is the signal detection. Coherent phonon displacement gives usually rise to very small changes in reflectivity, as they are only a tiny perturbation with respect to the equilibrium configuration in the crystal. Therefore, how to measure the signal is here the key point. The main point to extract the phonon signal from the reflectivity is to get rid of all sources of noise. Laser fluctuations can be accounted for by using a reference photodiode. We then measure the difference between the signal photodiode and the reference photodiode. In order to have a very high signal to noise ratio, a differential measurement coupled to a spectral filtering of the signal is required. This can be accomplished by using a chopper on the path of pump beam, which will therefore excite the sample at frequency lower than the probing pulse frequency. For example, for 1 kHz repetition rate laser, we use 500 Hz chopping frequency on the pump pulse. The difference between the signal and reference photodiodes is then analyzed by a lock-in amplifier at the pump chopping frequency. The lock-in amplifier produces a spectral filtering of the input signal, giving as an output signal only the changes in the reflectivity induced by the pump pulse. This is depicted in figure 3. This method results in a very high sensitivity. At 1 kHz laser repetition rate, we reach a signal to noise ratio of  $10^5$ , which is today the state of the art at this laser repetition rate (Boschetto, 2008, a). Moreover, using 80 MHz repetition rate it was possible to approach the shot noise limit of  $10^{-8}$ , which

allowed the detection of the vibrations of only two atomic thin layers of graphene (Boschetto, 2010 , b).

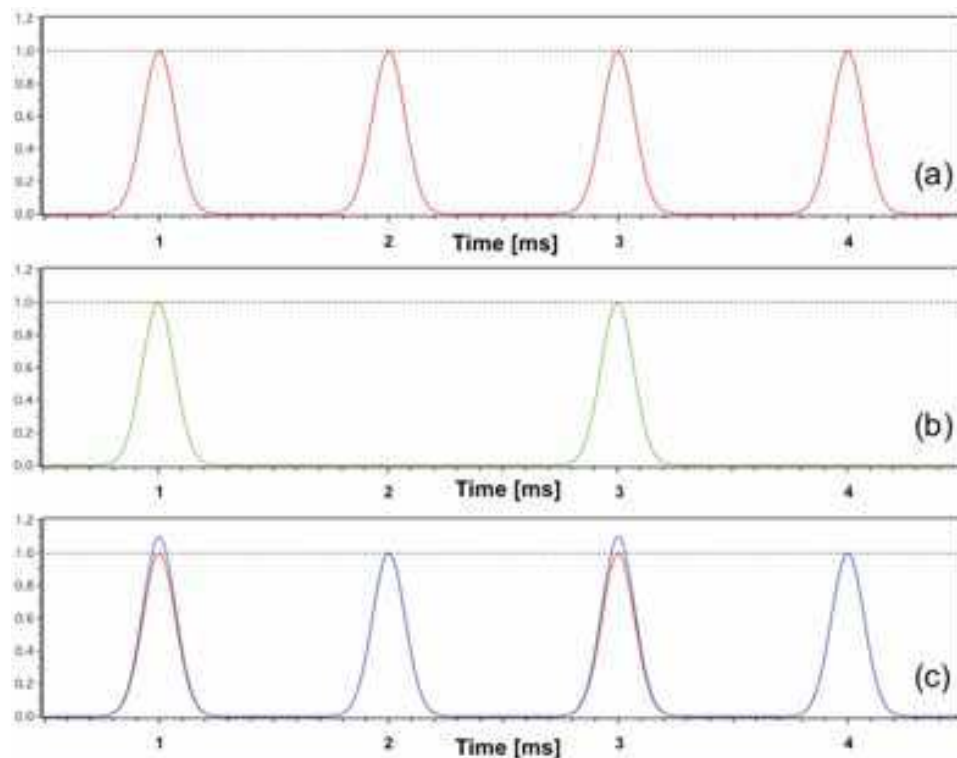


Fig. 3. Probe (a), pump (b) and pump perturbed probe (c) using a chopper at half the laser repetition rate.

#### 4. Bismuth crystal

The study of optical phonons in bismuth crystal is probably the most important from a pedagogical point of view. Actually, the elementary cell of bismuth contains only two atoms, displaced along the main diagonal of the cell (Boschetto, 2010 , a). Therefore, the study of the vibrational movement approaches a standard bookcase on harmonic oscillator, which is easier to understand. Within the bismuth structure, only two normal modes of vibration exist, namely the  $A_{1g}$  and the  $E_g$  mode. The  $A_{1g}$ , also called *breathing mode*, corresponds to the displacement of the atoms along the diagonal of the elementary cell, and remind the bookcase of standard harmonic oscillator. This mode of vibrations is also called "completely symmetric" because it preserves all the symmetry operations of the elementary cell. We note also that this displacement does not change the size of the elementary cell. The frequency of this mode, measured by Raman scattering process, is 2.92 THz, i.e. the vibration period is 342 fs (Lannin, 1975). This is a rather low frequency for optical phonon, basically because of the high atomic mass of bismuth, which is 209 u. The  $E_g$  mode corresponds to the displacement of the atoms in the plane perpendicular to the principal diagonal of the cell, and is therefore degenerate in the plane. This mode has an even lower frequency of 2.22 THz, corresponding to a vibrational period of 450 fs (Lannin, 1975). Any atomic movement within the elementary cell can be seen as superposition of these two normal modes. In contrast with its simple structure, bismuth has a very complex band structure and unique electronic properties (Edelman, 1977), which have intrigued the curiosity of scientists for decades. According to both experimental and theoretical results, valence and conduction band overlap only around a small region of the

Brillouin zone, allowing only a very small part of the electrons to be in the conduction band, which results in a low conductivity. However, it is interesting to note that electrons in bismuth can propagate over a long distance before experiencing any collision, giving rise to a quite large mean free path also at room temperature (Pippard, 1952).

## 5. Optical phonon in bismuth single crystal

Figure 4 shows a typical transient reflectivity in bismuth single crystal (Boschetto, 2008 , a), oriented along the  $[111]$  direction with respect to the trigonal elementary cell, corresponding to an excitation fluence of  $2.7 \text{ mJ/cm}^2$ . The oscillations due to the coherent  $A_{1g}$  optical phonon can clearly be seen, superimposed to a exponential like relaxation signal until a plateau is reached. The reflectivity recovers in around 4 ns. In figure 4, three different dynamics can be highlighted. Just after the excitation pulse arrival, the reflectivity increases because of the increase in electrons temperature. Besides, the coherent optical phonon oscillation is set up by this abrupt modification in electrons energy. While the lattice oscillates, the reflectivity decreases and passes through the zero in going toward negative value of the signal. This is due to a competition between the first two terms in equation 19. Indeed, for bismuth probed at 800 nm wavelength, reflectivity derivative calculations show that  $A_e > 0$  whereas  $A_L < 0$ . For positive time delay, while the electrons temperature decreases from its maximum value reached at  $t \sim 0$ , the lattice temperature increases due to electron phonon collisions. Therefore, the first two terms in equation 19 compete until the equilibrium is reached, at around 20 ps in our case, which is characterized by the plateau. For longer time delay, ranging in the 100 ps to ns range, the thermal diffusion is responsible for heat transfer out of the skin depth, resulting in a decrease in the crystal temperature at the surface. The red solid line in figure 4 correspond to a fit by the equation 19. Such a very good agreement was found for all the pump fluences ranging from 1 to  $25 \text{ mJ/cm}^2$ , which corresponds to the damage threshold we found experimentally.

The optical phonon parameters are strongly dependent on the pumping fluence, and this dependence gives important information on the crystal properties. We will focus our attention on the amplitude, frequency and damping time of the phonon. The amplitude generally increases linearly with the fluence. This is due to the fact that increasing the fluence results in both a larger number of free carriers as well as a stronger electrons temperature gradient, implying a bigger initial atomic displacement. Figure 5 shows an example of the phonon frequency in bismuth as a function of the pumping fluence. A small departure from the linear behavior is observed for fluences around  $15 \text{ mJ/cm}^2$ , close to the crystal damage threshold. This non linearity indicates that in this regime the atoms may displace in a stronger anharmonic regime.

On the other hand, increasing the fluence results in a red shift of the phonon frequency, as it can be observed in figure 6, in agreement with previous findings (DeCamp, 2001; Murray, 2005).

This can be explained again by the fact that increasing the fluence, the density of electrons excited into the conduction band increases as well, resulting in a softening of the interatomic bonding. This is a general observation in many materials, with the only exception so far known of  $V_2O_3$  (Mansart, 2010 , a) and graphite (Ischioka, 2008), in which the bonding are strengthen by the electrons excitation.

---

\*Readers may view, browse, and/or download material for temporary copying purposes only, provided these uses are for noncommercial personal purposes. Except as provided by law, this material

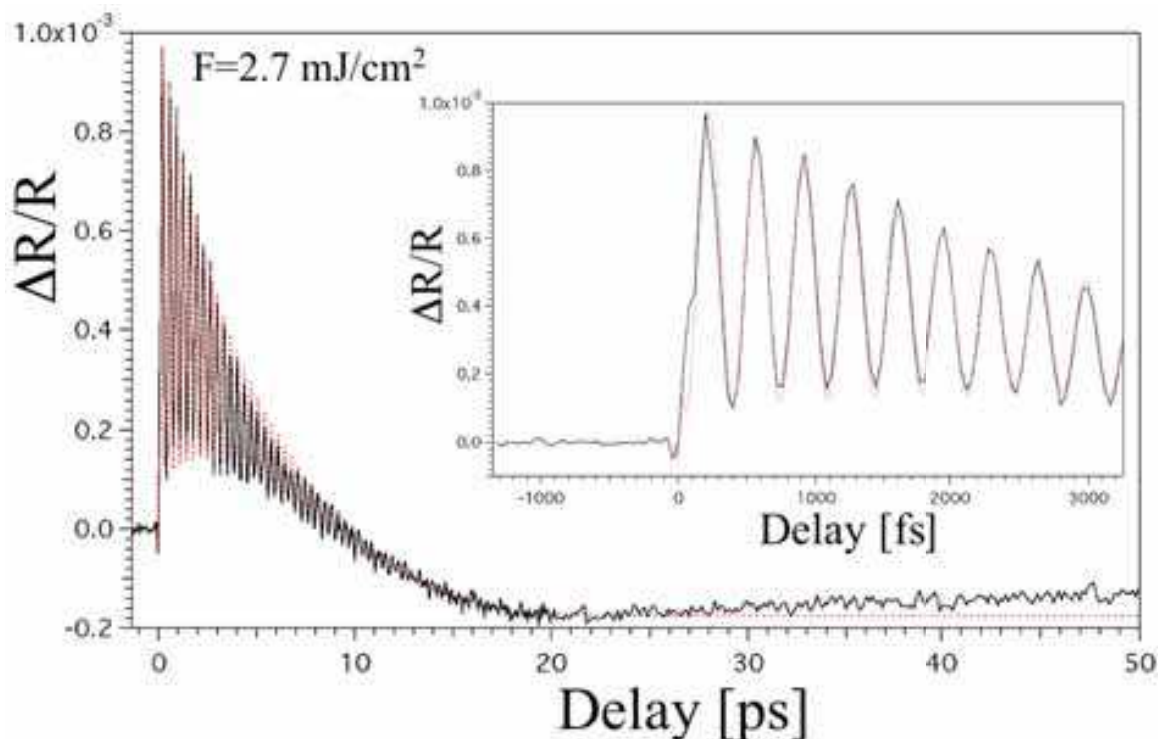


Fig. 4. Transient bismuth reflectivity at excitation fluence of  $2.7 \text{ mJ/cm}^2$ , reprinted with permission from (Boschetto, 2008 , a) (<http://prl.aps.org/abstract/PRL/v100/i2/e027404>), ©(2008) by the American Physical Society\*.

A closer look into the phonon frequency behavior shows a more sophisticated response. Actually, a more perfect adjustment of the phonon behavior highlights that the frequency of the oscillations is not constant and it rather depends on time delay (Hase, 2002). Therefore, a better insight into the change of phonon frequency versus the time delay, as depicted in figure 7. At time close to zero, the phonon frequency undergoes the largest red shift. Then, it relaxes back at its unperturbed value on a time scale that depends on the excitation fluence. This can be well understood by the fact that after the excitation by the pump pulse, the electrons relax back, therefore causing again the hardening of the atomic bonding. Figure 7 shows the time dependent evolution of phonon frequency for various pumping fluences. The initial softening followed by exponential relaxation is observed for any excitation fluence above  $4 \text{ mJ/cm}^2$ . For smaller fluence, the changes in frequency are within the error bars, and therefore cannot be investigated. Time resolved X-ray diffraction was successfully applied to the study of  $A_{1g}$  phonon in bismuth (Fritz, 2007), proving that the frequency red shift is mainly due to electronic softening of the interatomic potential.

The phonon damping constant  $\tau^{-1}$  also has a linear dependence versus the pumping fluence (Boschetto, 2008 , b), as shown in figure 8. The phonon damping time could be originated from both a decrease in phonon population or a dephasing in the oscillation. The coherent pump probe measurement does not allow to discriminate between these two possible effects. A pure dephasing implies simply a loss of coherence, even at constant phonons population. Instead, phonons population decay can have three main origins. First, the phonon population

may not be further reproduced, distributed, transmitted, modified, adapted, performed, displayed, published, or sold in whole or part, without prior written permission from the American Physical Society.

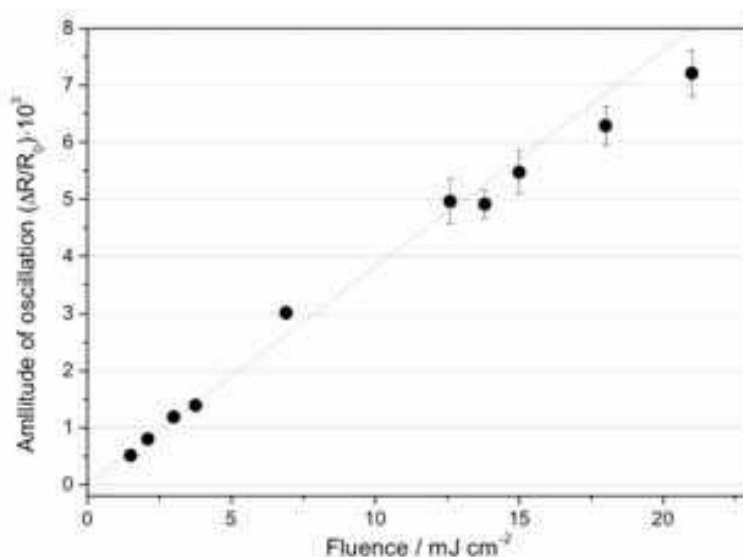


Fig. 5. Phonon amplitude versus pumping fluence (Garl, 2008 , a).

scattering, in which one phonon decays into two phonons, whose wavevectors and energy match both the energy and momentum conservation laws. This phonon-phonon transition is due to anharmonic effects, which introduces off diagonal terms in the phono- phonon interaction matrix, which would be pure diagonal in a perfect harmonic crystal. Of course, the strongest the anharmonicity, the higher is the transition probability between two different eigen modes. For example, in our case one optical phonon at the  $\Gamma$  point can be annihilated to produce two acoustical phonons outside the center of the Brillouin zone. Because of the momentum conservation, we cannot measure those acoustical phonons, and therefore we cannot monitor the phonon energy relaxation channel. The second possible reason for phonon damping is the electron phonon interaction. Actually, the electron phonon collisions implies energy and momentum exchange in both directions, from electrons to phonons and vice versa. Therefore, the excess energy stored in coherent phonons oscillation can be also lost in the interaction with the electrons. A third mechanism for phonon damping is scattering from impurities, which could also change the phase of oscillations.

### 5.1 Temperature dependence of optical phonon

The initial crystal temperature plays an important role in the measured phonon properties (Garl, 2008 , a;b). Figure 9 (a) shows the transient reflectivity for several initial crystal temperatures from 50 K up to 510 K, which is close to the melting point. Two main features can be highlighted. The phonon amplitude decreases whereas the phonon frequency undergoes a red shift when increasing the initial crystal temperature, as shown in the Fourier transform of the signal depicted in figure 9 (b).

The strong dependence of the coherent phonon amplitude on initial crystal temperature supports the scenario of excitation mechanism by DECP or TGM rather than a pure ISRS. This dependence could be explained as the following. The coherent optical phonon is generated by the increase in the free carriers density and/or the changes in electrons temperature, because of the gradient set up by the pump pulse. At very low temperature, the density of thermally excited electrons as well as their initial energy distribution is very low. The arrival of the pump pulse produces a larger modification with respect to the electrons initial conditions,

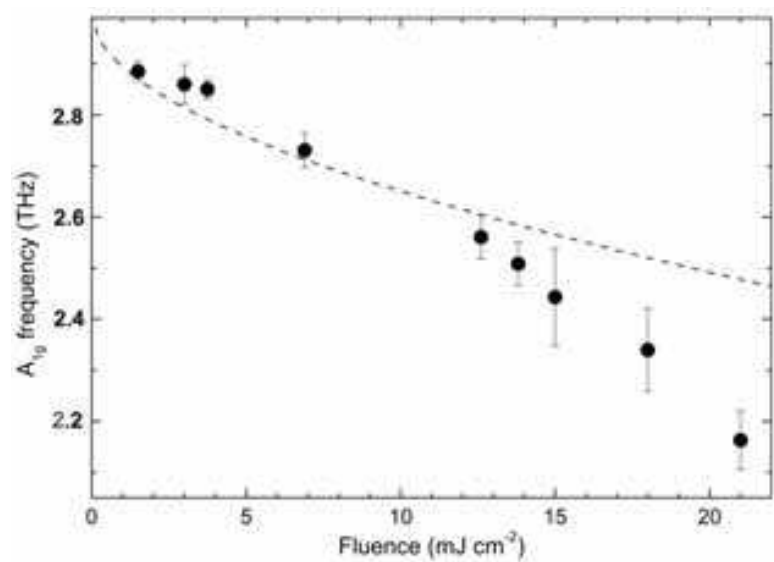


Fig. 6. Phonon frequency versus pumping fluence, reprinted with permission from (Garl, 2008 , b) (<http://prb.aps.org/abstract/PRB/v78/i13/e134302>), ©(2008) by the American Physical Society\*.

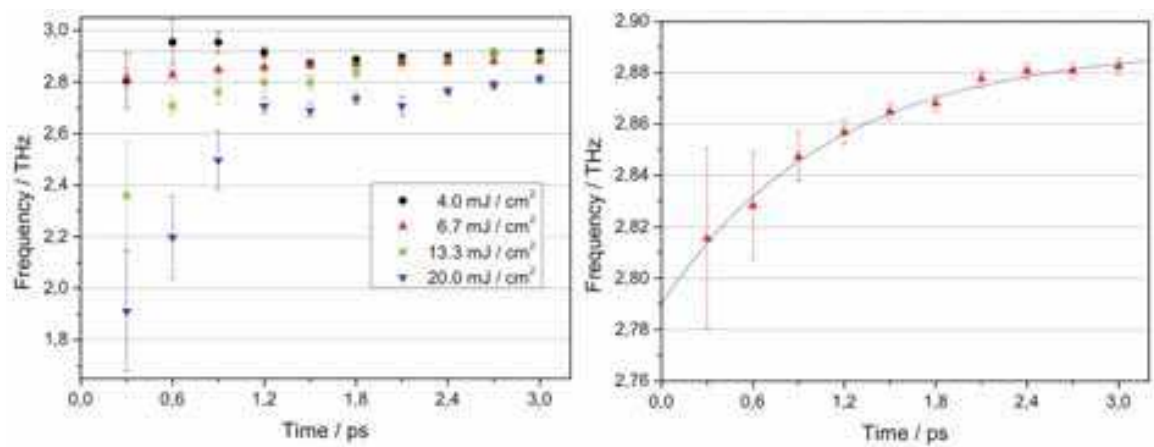


Fig. 7. Phonon frequency versus time delay (Garl, 2008 , a).

producing a larger coherent phonon amplitude. Therefore, at low temperature more energy can be stored in the coherent phonon displacement.

The behavior of the phonon frequency versus the temperature reinforces the scenario of bond softening by electrons excitations (Fritz, 2007). Actually, when increasing the temperature, the free carriers density increases, resulting in a softening of both atomic bonds and phonon frequency. This is in agreement with the results shown in the previous paragraph. The Fourier transform at 50 K shows also the existence of a secondary peak at 2.12 THz, which results in amplitude modulations of the  $A_{1g}$  optical phonon. This peak corresponds to the  $E_g$  optical mode, which can be observed only at very low temperature, as reported also by other teams (Ischioka, 2006). This mode is excited with a very low efficiency with respect to the  $A_{1g}$  mode.

5.2 Electrons and lattice temperatures in photoexcited bismuth crystal

In the previous paragraph we have explained the transient reflectivity in bismuth crystal by the competition of changes in both electrons and lattice temperatures superimposed to the

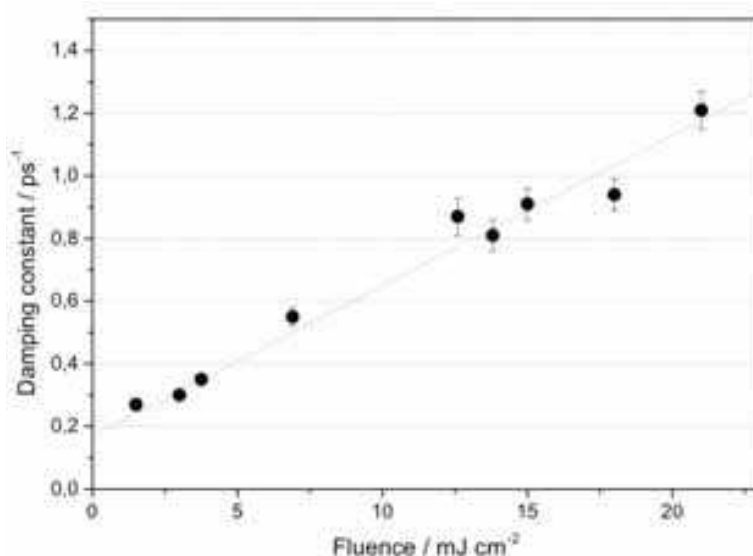


Fig. 8. Phonon damping constant versus fluence, reprinted with permission from (Garl, 2008 , b) (<http://prb.aps.org/abstract/PRB/v78/i13/e134302>), ©(2008) by the American Physical Society\*.

oscillations due to coherent optical phonon. The interesting question concerns the quantitative knowledge of both temperatures and their evolution in time. The final temperature at equilibrium, when the plateau is reached at around 20 ps, can be calculated by energy conservation neglecting the electrons diffusion. Knowing that the laser penetration depth in bismuth at 800 nm wavelength is 30 nm, the calculated final equilibrium temperature is then 1300 K, which must be compared to the melting temperature of 544 K. Obviously, this would mean that the plateau in reflectivity is rather due to either a transition of the crystal to liquid phase or a mixture of solid and liquid phase, instead of simple heating of the crystal as described by equation 19. In order to discriminate the formation of any liquid phase, we performed a double pump experiment (Boschetto, 2010 , a), with the second pump pulse arriving around 25 ps after the first pump pulse, shown in figure 10.

It can be clearly seen that the behavior of the reflectivity after the arrival of the second pump pulse is exactly the same as after the arrival of the first pump pulse. Moreover, the coherent phonon amplitude, frequency and damping time excited by the two pump pulses are nearly the same. This is a strong indication that there is no transition to liquid phase, neither any mixture of phase, otherwise the phonon parameters could not be the same.

## 6. Dielectric function measurement in bismuth single crystal

Reflectivity measurement gives only partial information about the transient state of the crystal, mainly because there is no direct link with the crystal structure and electronic configuration. Instead, we can gain a deeper understanding on the crystal dynamics under femtosecond photoexcitation by recovering the transient real and imaginary part of the dielectric function. There are mainly two ways to perform such a measurement, either the use of white light pulse combined to a spectrometer (Kudryashov, 2007), or using a double probe pulse at two known angles (Uteza, 2004). The former method gives access to a broad range response of the dielectric function, but it has a lower signal to noise ratio. Instead, by using a two probes set up, we can recover the dielectric function only for one wavelength at time, but



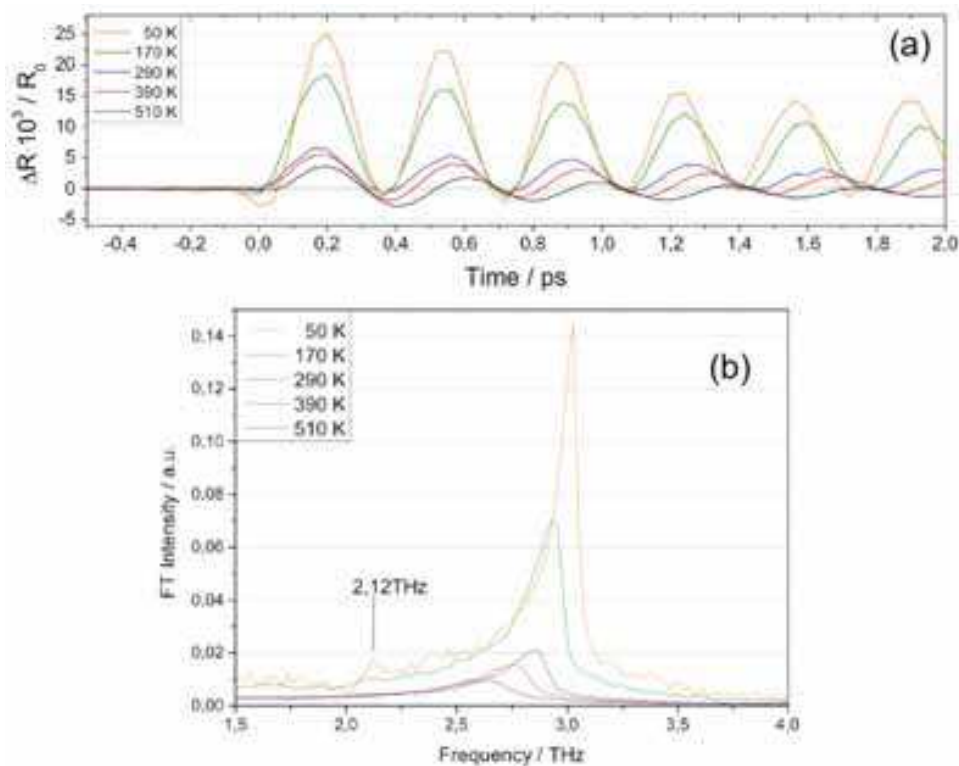


Fig. 9. Transient reflectivity (a) and its Fourier transform (b) for several initial crystal temperatures (Garl, 2008 , a).

the signal to noise ratio is much higher. The changes in reflectivity in photoexcited bismuth being very small, we had to use the second method. The real and imaginary part of dielectric constant are then recovered by using the Fresnel formulas. Figure 11 shows the transient behavior of the real and imaginary part of the dielectric constant at 800 nm in photoexcited bismuth (Garl, 2008 , a).

After the pump pulse arrival, we observe simultaneously an increase of the imaginary part and a decrease of the real part. This is consistent with the excitation of electrons in the conduction band, which enhances the conductivity. The coherent oscillations in both real and imaginary part shows that the electronic band structure is modulated by the coherent phonon displacement. This is not surprising because the excited phonon is at  $\Gamma$  point, and therefore the induced changes in interatomic distance concern the skin depth as whole. As the band structure depends also on the mean interatomic distance, its modulation will change periodically the electrons band structure as well. Instead, the relaxation behavior rises some question. When the plateau is reached, both the real and imaginary part are significantly different from the liquid phase value, as shown in the table 1 (Boschetto, 2010 , a). This confirms the aforementioned statement that when the equilibrium is reached, the skin depth is still in the solid state. This clearly indicates that the reached equilibrium temperature is well below the melting temperature, although the pumping energy density is higher than the enthalpy of melting.

This can be justified by the electrons transport out of the excited region. Actually, the very strong gradient set up by the pump pulse can be responsible of a fast electrons transport. Two main mechanisms could arise such a fast transport, namely the ballistic electrons transport and the electrons diffusion. The former takes place when the electron mean free path is longer then the skin depth. As the electrons Fermi velocity in bismuth reaches  $10^8\text{ cm/s}$  (Landolt,



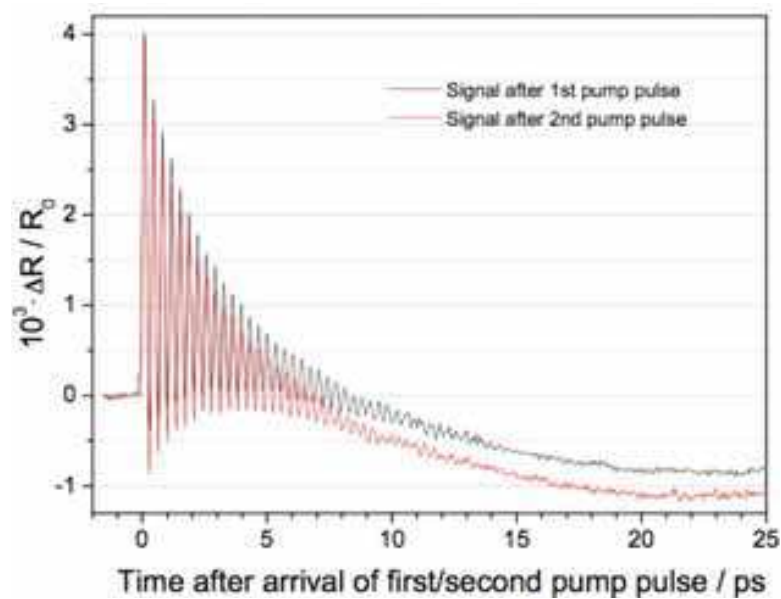


Fig. 10. Transient reflectivity of bismuth corresponding to double pump experiment, with the second pump arriving 25 ps after the first pump pulse, reprinted by permission of the publisher (Taylor & Francis Ltd, <http://www.tandf.co.uk/journals>) from (Boschetto, 2010 , a).

	$\epsilon_{Re}$	$\epsilon_{Im}$	$ \epsilon $
Solid	-16.25	15.40	22.39
Liquid	-11.0	28.9	30.92
Transient	-13.80	11.30	17.84

Table 1. Real and imaginary part of the dielectric function at 800 nm for the solid and liquid phase, as well as for the plateau of the transient reflectivity, reprinted by permission of the publisher (Taylor & Francis Ltd, <http://www.tandf.co.uk/journals>) from (Boschetto, 2010 , a).

2006), the excited electrons would leave the skin depth on a time scale comparable with the pulse duration. This would imply that the skin depth temperature does not change, in contrast with previous observations. Instead, diffusive transport is a much slower process, which takes place when the electrons mean free path is small in comparison to the skin depth. Using the equations 12 and taking into account the electrons thermal conductivity, we found at equilibrium a temperature increase of only 20 K. The final lattice temperature can also be calculated by using the known changes in reflectivity toward the crystal temperature (Wu, 2007), as well as by using the coherent optical phonon parameters dependence on initial crystal temperature (Garl, 2008 , a). All these methods give around the same value of the temperature rise.

The scenario of fast electrons transport is further supported by the comparison with recent experiments by time resolved electrons diffraction on 30 nm bismuth thin film (Sciaini, 2009), in which a pump fluence of 1.3 mJ/cm<sup>2</sup> was enough to produce a transition to the liquid phase. Actually, in thin film the electrons cannot propagate in the direction of the temperature gradient, and their confinement results in a larger increase in the lattice temperature. Instead, in our case we used bulk crystal, in which there is no confinement of electrons.

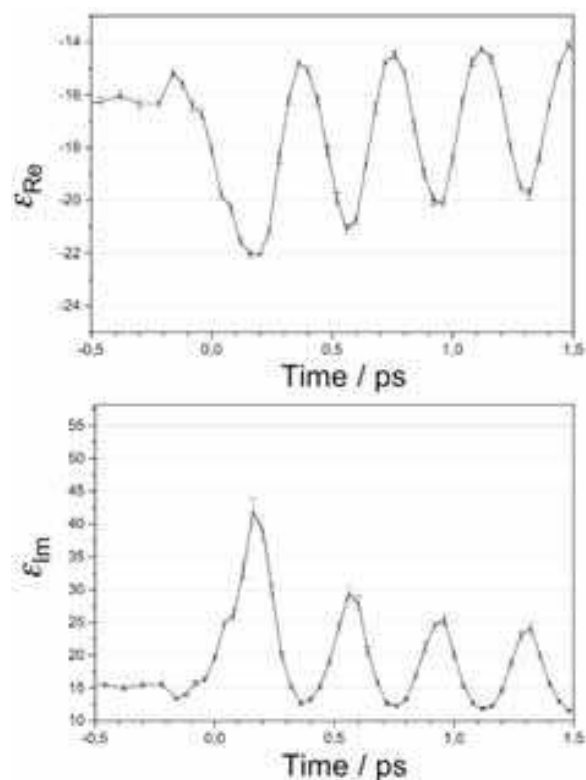


Fig. 11. Transient dielectric function of photoexcited bismuth (Garl, 2008 , a).

In order to further investigate the dynamics of electrons and lattice in photoexcited bismuth, the dielectric function should be recovered in a larger spectral range. This would also give access to the modifications in the electrons band structure and its correlation with the coherent phonon mode.

## 7. Coherent optical phonon in strongly correlated materials

A great interest in studying coherent optical phonons is obviously in those materials in which electrons and lattice are strongly coupled, as well as in materials where the lattice displacements may play a role in the phase transitions. The strongly correlated materials are a large class of materials that often meet these conditions and in which the interplay between all the degrees of freedom of the crystal such as spin, charge and lattice gives rise to exotic phase diagrams. This subtle equilibrium can be strongly perturbed by the external laser pulse, leading sometimes to new phases. For example, in a manganite crystal it has even been shown that a phase transition can be induced by a coherent phonon in absence of resonant absorption (Rini, 2007). Among the strongly correlated electrons materials, the  $V_2O_3$  crystal is of primary importance, as it is the prototype of Mott transition. Time resolved measurements on this compound have shown the excitation of both coherent acoustic and optical phonons (Mansart, 2010 , a). Interestingly, the laser pulse excitation produces a stiffening of the coherent  $A_{1g}$  mode. This indicates that the electrons excitation by the pump laser pulse gives rise to a hardening of the atomic bonding, in contrast with the softening in other materials like bismuth. Recently, the attention of a large part of the international community working on superconductors has been focussed on iron pnictides, which are new compounds showing interesting phase diagram and high superconductivity transition temperature. The coherent phonon study in the pnictide  $Ba(Fe_{1-x}Co_x)_2As_2$  (Mansart, 2009) has suggested that

the  $A_{1g}$  mode does not participate to the phase transition. These results have also allowed the evaluation of the electrons phonon coupling constant (Mansart, 2010 , b), as well as to invalidate the Bardeen-Cooper-Schrieffer theory as origin of the superconductivity in this material. We point out here that the coherent phonon spectroscopy is the key approach to determine the electron phonon coupling constant of a given phonon mode.

The extension of coherent phonon studies to many other processes can be reached also by the development of tunable sources in a large spectral range. Especially, the advance in both femtosecond X-ray sources and in THz sources will allows a deeper insight in the correlations between the phonons and the physical properties in many materials.

## 8. Conclusions

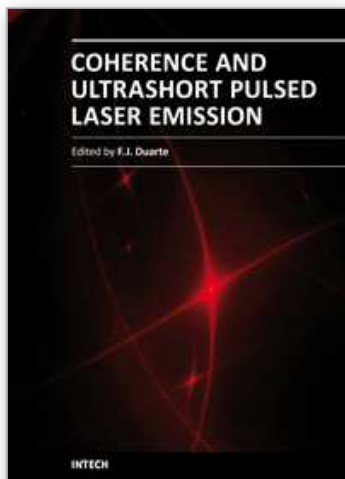
In conclusions, in this chapter we have suggested how to approach the study of coherent optical phonon, focussing our attention on the pedagogical case of bismuth. We have shown that it is possible to control selectively the atomic displacement corresponding to one phonon mode. The study of the  $A_{1g}$  mode in bismuth has revealed some general properties of the coherent optical phonon as function of the pump pulse excitation as well as of the initial crystal temperature. As the changes in reflectivity gives only partial information on the electrons and phonon dynamics, we have shown the use of double probe pulse to recover the transient behavior of the real and imaginary part of the dielectric function. This study has demonstrated that the excess energy brought by the pump pulse is transported away from the skin depth by fast electrons diffusion, preventing any formation of liquid phase. We have discussed some examples of coherent phonon studies in strongly correlated electrons materials and shown that investigating coherent phonon dynamics will allow to gain fundamental knowledges on the physical properties of many materials.

## 9. References

- Anisimov, S. I. et al. (1975). Electron emission from metal surfaces exposed to ultrashort laser pulses. *Sov. Phys. JETP*, Vol. 39, No. 2, August 1974, 375-377.
- Ashcroft, N. W. Mermin, N. D. (1976). *Solid State Physics*, Saunders College, ISBN 0-03-083993-9, New York, New York, United States of America.
- Beaud, P. et al. (2007). Spatiotemporal Stability of a Femtosecond HardX-Ray Undulator Source Studied by Control of Coherent Optical Phonons. *Physical Review Letters*, Vol. 99, October 2007, 174801.
- Boschetto, D. et al (2008). Small Atomic Displacements Recorded in Bismuth by the Optical Reflectivity of Femtosecond Laser-Pulse Excitations. *Physical Review Letters*, Vol. 100, January 2008, 027404.
- Boschetto, D. et al (2008). Lifetime of optical phonons in fs-laser excited bismuth. *Applied Physics A*, Vol. 92, May 2008, 873-876.
- Boschetto, D. et al (2010). Ultrafast dielectric function dynamics in bismuth. *Journal of Modern Optics*, Vol. 57, Issue No. 11, 20 June 2010, 953-958.
- Boschetto, D. et al (2010). Coherent interlayer vibrations in bilayer and few-layer graphene. *Submitted*.
- Boyd, R. W. (2003). *Nonlinear Optics*, Academic Press, ISBN 0-12-121682-9, San Diego, California, United States of America.
- DeCamp, M. F. et al. (2001). Dynamics and coherent control of high amplitude optical phonons in bismuth. *Physical Review B*, Vol. 64, August 2001, 092301.

- Edelman, V. S. (1977). Properties of electrons in bismuth. *Sov. Phys. Usp.*, Vol. 20, October 1977, 819-835.
- Fritz, D. M. et al. (2007). Ultrafast bond softening in bismuth: mapping a solid's interatomic potential with X-rays. *Science*, Vol. 315, February 2007, 633-636.
- Garl, T. (2008). Ultrafast Dynamics of Coherent Optical Phonons in Bismuth, *PhD thesis*, July 2008, Ecole Polytechnique.
- Garl, T. et al. (2008). Birth and decay of coherent optical phonons in femtosecond-laser-excited bismuth, *Physical Review B*, Vol. 78, October 2008, 134302.
- Hase, M. et al. (2002). Dynamics of Coherent Anharmonic Phonons in Bismuth Using High Density Photoexcitation. *Physical Review Letters*, Vol. 88, No. 6, January 2002, 067401.
- Ishioka, K. et al. (2006). Temperature dependence of coherent  $A_{1g}$  and  $E_g$  phonons of bismuth. *Journal of Applied Physics*, Vol. 100, November 2006, 093501.
- Ishioka, K. et al. (2008). Ultrafast electron-phonon decoupling in graphite. *Physical Review B*, Vol. 77, March 2008, 121402.
- Kudryashov, S. I. et al. (2007). Intraband and interband optical deformation potentials in femtosecond-laser-excited alpha-Te. *Physical Review B*, Vol. 75, February 2007, 085207.
- Landolt-Börnstein (2006). Numerical Data and Functional Relationships in Science and Technology. Edited by O. Madelung, U. Rössler, and M. Schulz, *Landolt-Börnstein*, New Series, Group III, Vol. 41C (Springer-Verlag, Berlin, 2006).
- Lannin, J. S. et al. (1975). Second order Raman scattering in the group  $V_b$  semimetal Bi Sb and As. *Physical Review B*, Vol. 12, No. 2, July 1975, 585-593.
- Mansart, B. et al. (2009). Observation of a coherent optical phonon in the iron pnictide superconductor  $Ba(Fe_{1-x}Co_x)_2As_2$  ( $x = 0.06$  and  $0.08$ ). *Physical Review B*, Vol. 80, (November 2009), 172504.
- Mansart, B. et al. (2010). Ultrafast dynamical response of strongly correlated oxides: role of coherent optical and acoustic oscillations. *Journal of Modern Optics*, Vol. 57, June 2010, 959-966.
- Mansart, B. et al. (2010). Ultrafast transient response and electron-phonon coupling in the iron-pnictide superconductor  $Ba(Fe_{1-x}Co_x)_2As_2$ . *Physical Review B*, Vol. 82, July 2010, 024513.
- Merlin, R. (1997). Generating coherent THz phonons with light pulses. *Solid State Communications*, Vol. 102, No. 2-3, 1997, 207-220.
- Murray, E. D. et al. (2005). Effect of lattice anharmonicity on high-amplitude phonon dynamics in photoexcited bismuth. *Physical Review B*, Vol. 72, August 2005, 060301.
- Papalazarou, E. et al. (2008). Probing coherently excited optical phonons by extreme ultraviolet radiation with femtosecond time resolution, *Applied Physics Letters*, Vol. 93, July 2008, 041114.
- Pippard, A. B., et al. (1952). The Mean Free Path of Conduction Electrons in Bismuth. *Proceedings of Royal Society A*, Vol. 65, August 1952, 955-956.
- Rini, M. et al. (2007). Control of the electronic phase of a manganite by mode-selective vibrational excitation. *Nature*, Vol. 449, September 2007, 72-74.
- Rousse, A., et al. (2001). Non-thermal melting in semiconductors measured at femtosecond resolution. *Nature*, Vol. 410, March 2001, 65-68.
- Sciaini, G. et al. (2009). Electronic acceleration of atomic motions and disordering in bismuth. *Nature*, Vol. 458, March 2009, 56-59.
- Sokolowski-Tinten, K. et al. (2003). Femtosecond X-ray measurement of coherent lattice vibrations near the Lindemann stability limit. *Nature*, Vol. 422, March 2003, 287-289.

- Stevens, T. E. et al. (2002). Coherent phonon generation and the two stimulated Raman tensors. *Physical Review B*, Vol. 65, March 2002, 144304.
- Uteza, O. P. et al. (2004). Gallium transformation under femtosecond laser excitation: Phase coexistence and incomplete melting. *Physical Review B*, Vol. 70, August 2004, 054108.
- Yan, Y.-X. et al. (1985). Impulsive stimulated Raman scattering: General importance in femtosecond laser pulse interaction with matter, and spectroscopy applications. *Journal of Chemical Physics*, Vol. 83, 1985, 5391-5399.
- Wu, A. Q. et al. (2007). Coupling of ultrafast laser energy to coherent phonons in bismuth. *Applied Physics Letters*, Vol. 90, June 2007, 251111.
- Zeiger, H.J. et al. (1992). Theory for displacive excitation of coherent phonons. *Physical Review B*, Vol. 45, January 1992, 768-778.
- Ziman, J. M. (2004). *Electrons and Phonons*, ISBN 0-19-850779-8, Oxford University Press, New York, United States of America.



## **Coherence and Ultrashort Pulse Laser Emission**

Edited by Dr. F. J. Duarte

ISBN 978-953-307-242-5

Hard cover, 688 pages

**Publisher** InTech

**Published online** 30, November, 2010

**Published in print edition** November, 2010

In this volume, recent contributions on coherence provide a useful perspective on the diversity of various coherent sources of emission and coherent related phenomena of current interest. These papers provide a preamble for a larger collection of contributions on ultrashort pulse laser generation and ultrashort pulse laser phenomena. Papers on ultrashort pulse phenomena include works on few cycle pulses, high-power generation, propagation in various media, to various applications of current interest. Undoubtedly, Coherence and Ultrashort Pulse Emission offers a rich and practical perspective on this rapidly evolving field.

### **How to reference**

In order to correctly reference this scholarly work, feel free to copy and paste the following:

Davide Boschetto and Antoine Rousse (2010). Coherent Optical Phonons in Bismuth Crystal, Coherence and Ultrashort Pulse Laser Emission, Dr. F. J. Duarte (Ed.), ISBN: 978-953-307-242-5, InTech, Available from: <http://www.intechopen.com/books/coherence-and-ultrashort-pulse-laser-emission/coherent-optical-phonons-in-bismuth-crystal>

**INTECH**  
open science | open minds

### **InTech Europe**

University Campus STeP Ri  
Slavka Krautzeka 83/A  
51000 Rijeka, Croatia  
Phone: +385 (51) 770 447  
Fax: +385 (51) 686 166  
[www.intechopen.com](http://www.intechopen.com)

### **InTech China**

Unit 405, Office Block, Hotel Equatorial Shanghai  
No.65, Yan An Road (West), Shanghai, 200040, China  
中国上海市延安西路65号上海国际贵都大饭店办公楼405单元  
Phone: +86-21-62489820  
Fax: +86-21-62489821

© 2010 The Author(s). Licensee IntechOpen. This chapter is distributed under the terms of the [Creative Commons Attribution-NonCommercial-ShareAlike-3.0 License](https://creativecommons.org/licenses/by-nc-sa/3.0/), which permits use, distribution and reproduction for non-commercial purposes, provided the original is properly cited and derivative works building on this content are distributed under the same license.

IntechOpen

IntechOpen